Kovove Mater. 49 2011 307–318
DOI: 10.4149/km_2011_5_307

Constant structure creep experiments on aluminium

K. Milička†

Institute of Physics of Materials, Academy of Sciences of the Czech Republic, Žižkova 22, 616 62 Brno, Czech Republic

Received 25 February 2011, received in revised form 25 March 2011, accepted 25 March 2011

Abstract

Creep behaviour of pure aluminium was investigated using constant structure creep experiments performed in the steady-state creep stage over a wide temperature interval from 523 to 773 K. The simultaneous activity of two parallel operating dislocation mechanisms was deduced from an analysis of the experiments. Both mechanisms are probably governed by diffusion along dislocation cores; however, they differ substantially in their activation areas. The contributions of the mechanisms to the steady-state creep rate depend on the applied stress and temperature. The nature of both mechanisms is extensively discussed.

K e y w o r d s: mechanical properties, high temperature deformation, creep, aluminium

1. Introduction

Conventional analysis of the creep deformation behaviour of metallic materials at elevated temperatures and fundamental investigations of creep mechanisms governing this behaviour were mostly based on analyses of the applied stress and temperature dependence of the steady-state creep rate obtained from a suitable set of creep curves. However, in all conventional procedures of the analysis of creep as a thermally activated process, a crucial problem is the elimination of influences of structure differences corresponding to the steady-state under various applied stresses σ and temperature T. If such influences cannot be fully determined or eliminated, the activation parameters resulting from such analyses should be taken, in principle, as phenomenological quantities only. Thus, they must be judged carefully in any physical explanation of the specific mechanisms controlling the creep of a given metal or alloy. In order to resolve these complicating problems, alternative procedures for the analysis of creep behaviour have been applied, which allow either the elimination or reduction of the influences of different structure states corresponding to the steady-state creep rate under various external conditions. Procedures based on the constant structure experiments in creep (in what follows, CSC) have been applied by several authors over the last two decades [1–5].

In principle, all CSC experiments are based on sudden changes in testing conditions, i.e., either the applied stress or temperature – and of the analysis of the immediate strain response to such a change. The fundamental idea of this analysis is based on the assumption that both structure states immediately before and after the change are either identical or their differences are not substantial. As the quantity, which characterises the response, the immediate deformation rate $\dot{\varepsilon}_r$ after the change is most often taken into consideration. This rate and the creep rate immediately before the change correspond to an identical structure but to different external conditions. Sudden changes of applied stress are preferred in the CSC experiments because they are easier to perform. Sudden changes of temperature can be experimentally very difficult to perform and have been applied rarely.

Aluminium has been extensively used as an academic material in the course of the development of a

† Karel Milička passed away on the 25th February 2010 after a short battle with cancer. The paper emerged in his collection of manuscripts, prepared for submission but unfortunately not expedited. The final manuscript was revised by Ferdinand Dobeš* of the same institute.

*Corresponding person: tel.: +420 532 290 408; e-mail address: dobes@ipm.cz

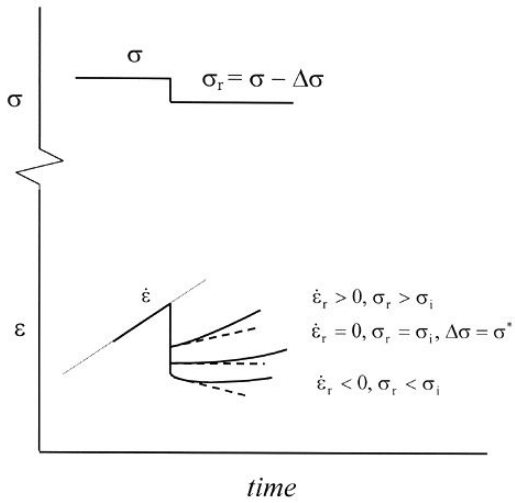

Fig. 1. Illustrations of strain responses to various applied stress reductions $\Delta\sigma$ performed in the course of creep.

fundamental understanding of creep in metallic materials. A great number of models and theories of high temperature creep in pure metals have been demonstrated through their applications to the creep data of this material. It is understandable that aluminium has also been used in the CSC experiments, e.g. [1–3].

In the opinion of the present author, not all the possibilities for the application of CSC procedure have been explored. Thus, further investigations of the CSC phenomena were performed using pure aluminium in order to broaden knowledge of the phenomena and its application in basic studies.

2. Constant structure creep experiments and their interpretation

After a sudden applied stress reduction $\sigma \rightarrow \sigma - \Delta\sigma = \sigma_r$ performed in the course of a creep test, three different shapes of the immediate strain response can be observed (Fig. 1). At a small $\Delta\sigma$, the forward creep rate $\dot{\varepsilon}_r$ is observed immediately after the instantaneous shortening of the specimen. For a certain $(\Delta\sigma)_o$, a zero creep rate $\dot{\varepsilon}_r$ follows and, at higher values of $\Delta\sigma$, negative, i.e., backward rate $\dot{\varepsilon}_r$ can be seen after the reduction. Pursuant to such an observation, Ahlquist and Nix [6] suggested the strain transient dip test technique for measuring effective and internal stresses in creep. The rate $\dot{\varepsilon}_r$ is considered to be the result of the confrontation of the residual applied stress σ_r acting after the stress reduction and the internal stress σ_i in crept material. A positive rate $\dot{\varepsilon}_r$ is observed if $\sigma_r > \sigma_i$, a negative $\dot{\varepsilon}_r$ corresponds to $\sigma_r < \sigma_i$, and zero $\dot{\varepsilon}_r$ means that these stresses are equal. The effective stress σ^* is then

$$\sigma^* = (\Delta\sigma)_{\dot{\varepsilon}_r=0} = \sigma - \sigma_i. \tag{1}$$

The common assumption accepted in all CSC experiments is that the rate $\dot{\varepsilon}_r$ corresponds to the same state of structure as exists in the crept material immediately before the stress change. The difference in various interpretations of the rate $\dot{\varepsilon}_r$ lies in the choice of which stress variable is considered to be decisive for the value of this rate. In practice, three approaches have been so far suggested.

In the first approach, the reference stress for the CSC rate $\dot{\varepsilon}_r$ is the residual applied stress $\sigma_r = \sigma - \Delta\sigma$ or its normalized value σ_r/σ. The relevant procedures are similar to the conventional procedures for the analysis of the applied stress dependence of the steady-state creep rate $\dot{\varepsilon}_s$. This approach was used to estimate the influence of subgrain size on the applied stress dependence of creep rate [7] and for an analysis of the creep behaviour of aluminium and its solid solution [1, 2]. The basic problem with this approach is the explanation of negative CSC rates $\dot{\varepsilon}_r$, which are observed at the positive residual applied stresses σ_r. Therefore, for this interval of the stresses σ_r, Vogler et al. [1] had to define the CSC rate in a modified manner.

The second approach, suggested by Nakayama and Gibeling [3] and also extensively discussed by Dobeš [4], is based on the applications of dislocation kinetics and thermodynamics. Briefly, the decisive stress is the residual applied stress σ_r and the dependence of the rate $\dot{\varepsilon}_r$ on this stress is given by the kinetic law [8] whose simplified form is [3]

$$\dot{\varepsilon}_r \propto \exp\left[-\frac{\Delta F}{kT}\left(1-\frac{\sigma_r}{\hat{\tau}}\right)\right], \tag{2}$$

where ΔF is the total Helmholtz free energy of the obstacle for dislocation motion and the stress $\hat{\tau}$ characterises the friction stress of the structure prior to the stress reduction. The relationship was applied over a relative small interval of residual stresses $\sigma_r < \sigma$. However, the application on creep of aluminium yielded questionable conclusions concerning the value of the energy ΔF [9]. Note that the negative rates $\dot{\varepsilon}_r$ cannot be described by Eq. (1).

Milička [5] considers the residual effective stress σ_r^*, defined as

$$\sigma_r^* = \sigma^* - \Delta\sigma, \tag{3}$$

the stress variable relevant for the value of the CSC rate $\dot{\varepsilon}_r$. Thus, the original and rather qualitative assumption of Ahlquist and Nix [6] is applied quantitatively. Suitably, the stress σ_r^* is positive over the whole region of the reductions $\Delta\sigma$ at which the positive rates

$\dot{\varepsilon}_\mathrm{r}$ are observed and it is negative at the negative rates $\dot{\varepsilon}_\mathrm{r}$. In this way, the fundamental problem of previous approaches is resolved.

CSC experiments have mostly been performed over the range of the steady-state creep region. Generally, it is assumed that structure can be considered constant over this whole creep region. From a theoretical point of view, it can be assumed that a general equation of the state

$$\dot{\varepsilon} = f\left(\sigma,T,S_1,\ldots S_n\right), \quad S_j \; - \; \text{structure variables} \tag{4}$$

is valid also for the creep rate $\dot{\varepsilon}_\mathrm{s}$. While the applied stress σ and temperature T are constant for a given creep test, it can also be expected that all relevant variables S_j are constant over the whole steady-state range. Thus, if only short-term stress reductions are performed in the steady-state creep and then, after the reloading of the test on the nominal stress σ, the creep rate quickly reaches the value of $\dot{\varepsilon}_\mathrm{s}$, a set of the stress reductions can be performed with various $\Delta\sigma$. In such a way, a suitable set of data $\dot{\varepsilon}_\mathrm{r} = \dot{\varepsilon}\left(\Delta\sigma\right)$ is obtained in a single or in a few of creep tests with identical or nearly identical steady-state creep rate $\dot{\varepsilon}_\mathrm{s}$ at given σ and T.

The CSC data $\dot{\varepsilon}_\mathrm{r} = \dot{\varepsilon}\left(\Delta\sigma\right)$ can be very well described in several metallic materials by simple sinh relationship [5]:

$$\dot{\varepsilon}_\mathrm{r} = A \sinh\left[B\sigma_\mathrm{r}^*\right], \tag{5}$$

where parameters A and B depend on the external condition, i.e., the applied stress σ and temperature at which the steady-state creep occurs. In addition to the assumptions of the constant internal stress and the decisive role of the stress σ_r^* during the stress change, Milička [5] also assumes the inalterability of mechanisms that control and cause creep deformation before and after the stress change including inalterability of their activation areas a^*. Further, the mean rate of dislocation motion v can be generally expressed as

$$v = v_\mathrm{o} \exp\left[-\frac{\Delta F}{RT}\right] \sinh\left[\frac{a^* b \sigma_\mathrm{r}^*}{RT}\right], \tag{6}$$

where factor v_o and the Helmholtz energy ΔF do not depend on the stress σ_r^*; b is the Burgers vector length, R is the gas constant. The validity of this expression and the Orowan equation

$$\dot{\varepsilon} \propto \rho_\mathrm{m}^\mathrm{s}\, b\, v, \tag{7}$$

($\rho_\mathrm{m}^\mathrm{s}$ is density of moving dislocation in the steady--state region) results in close relationships between the parameters A and B and characteristics of the creep mechanism acting in the steady-state creep region, i.e.,

$$A \propto v_\mathrm{o}\, \rho_\mathrm{m}^\mathrm{s} \exp\left[-\frac{\Delta F}{RT}\right] \tag{8}$$

and

$$B = \frac{a^* b}{RT}. \tag{9}$$

The investigations of CSC dependence in the primary creep region require much more experimental effort [10]. The investigations in several metals and alloys have shown that the CSC dependence $\dot{\varepsilon}_\mathrm{r} = \dot{\varepsilon}_\mathrm{r}(\Delta\sigma)$ can be very well described as the sum of two functions; the form of each can be described by an equation similar to Eq. (5). Thus, the primary creep can be considered the result of two mechanisms with the role of one progressively decreasing and becoming quite minor in the steady-state region [10].

3. Experimental

Aluminium of purity 4N was used for the experiments. From an ingot, 10 mm thick strips were rolled. Cylindrical specimens with a 50 mm gauge length and 6 or 7 mm in cross-section diameter, respectively, were machined. The longitudinal axes of the specimens were parallel with the rolling direction of the strips. Finally, the specimens were annealed in evacuated silica ampoules at 773 K for 24 h and then air-cooled. From such treatment, a uniform grain size resulted, with an average value of 0.2 mm.

Investigations of creep behaviour consisted of isothermal constant stress tensile creep tests and constant structure creep experiments. The tests were performed in a protective argon atmosphere. The elongation of the specimens was measured by the LVTD Hottinger-Baldwin Measurements set KWS3073 + W5K, enabling high-resolution measurements, and it was continuously recorded by a computer. The frequency of readings during strain transients in the CSC experiments varied from 10 to 14 Hz, depending on the digital multimeter used.

Creep curves and all important creep characteristics were very well reproducible over the whole range of testing conditions. The CSC experiments were performed in the steady-state creep regions of the tests. As a rule, the strain of these creep regions was large enough and allowed the determination of the whole dependence $\dot{\varepsilon}_\mathrm{r} = \dot{\varepsilon}_\mathrm{r}(\Delta\sigma)$ in one or two tests. In all stress reductions, the time interval of strain recording uncertainty, resulting from a finite rate of unloading, from elastic vibrations of the equipment and from the limited rate of the elongation record, did not exceed 0.4 s (usually 0.2 s). In each single-specimen CSC experiment, each subsequent stress reduction

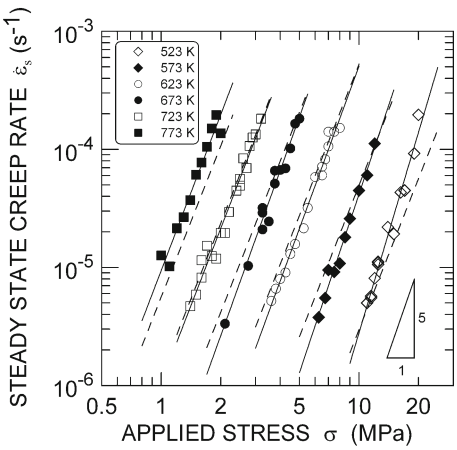

Fig. 2. Dependence of the steady-state creep rate on the applied stress at experimental temperatures.

was performed whenever the creep rate after the reloading to nominal applied stress σ reached the original value of $\dot{\varepsilon}_\mathrm{s}$; the interval $\Delta\varepsilon$ between two subsequent changes was generally greater than 0.002. The experimental equipment enables the ascertaining of the $\dot{\varepsilon}_\mathrm{r}(\Delta\sigma)$ dependence in the range of the steady-state creep rate $\dot{\varepsilon}_\mathrm{s}$ from $2\times10^{-6}\,\mathrm{s}^{-1}$ to $4\times10^{-4}\,\mathrm{s}^{-1}$. The choice of creep conditions corresponds to the situation where dislocation creep is assumed to be the dominant type of creep process. A set of special software was developed for the determination of the CSC rate $\dot{\varepsilon}_\mathrm{r}$ from records of strain responses to stress changes.

4. Results

4.1. Applied stress and temperature dependence of steady-state creep rate

The dependence of the steady-state creep rate $\dot{\varepsilon}_\mathrm{s}$ on the applied stress and temperature is plotted in Fig. 2. Points plotted in the figure correspond to the external conditions at which the CSC experiments were performed in the steady-state region. The applied stress sensitivity parameter n of the rate $\dot{\varepsilon}_\mathrm{s}$, defined as

$$n = \left(\frac{\partial \ln \dot{\varepsilon}_\mathrm{s}}{\partial \ln \sigma}\right)_\mathrm{T}, \tag{10}$$

reaches values close to 4.5 for all experimental temperatures. The description of the combined temperature and applied stress dependence of the rate $\dot{\varepsilon}_\mathrm{s}$ by a frequently used simple function

$$\dot{\varepsilon}_\mathrm{s} = K\sigma^m \exp\left[-\frac{Q_\mathrm{SS}}{RT}\right] \tag{11}$$

has yielded optimum values $m = 4.25 \pm 0.18$ and $Q_\mathrm{SS} = 168 \pm 6\,\mathrm{kJ\,mol^{-1}}$. The value of the energy Q_SS is somewhat greater than the activation enthalpy of lattice diffusion $\Delta H \approx 144\,\mathrm{kJ\,mol^{-1}}$, e.g. [11]. Dashed lines in Fig. 2 illustrate the applicability of such description of the dependences.

4.2. Constant structure creep experiments

Examples of strain responses to various applied stress changes are illustrated in Fig. 3. The extent

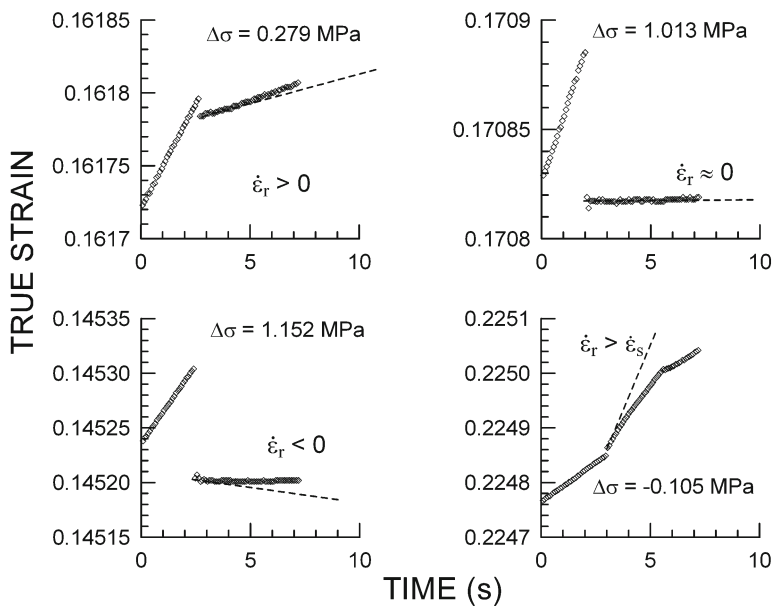

Fig. 3. Examples of the strain response to applied stress changes, test at 723 K, $\sigma = 2.2$ MPa.

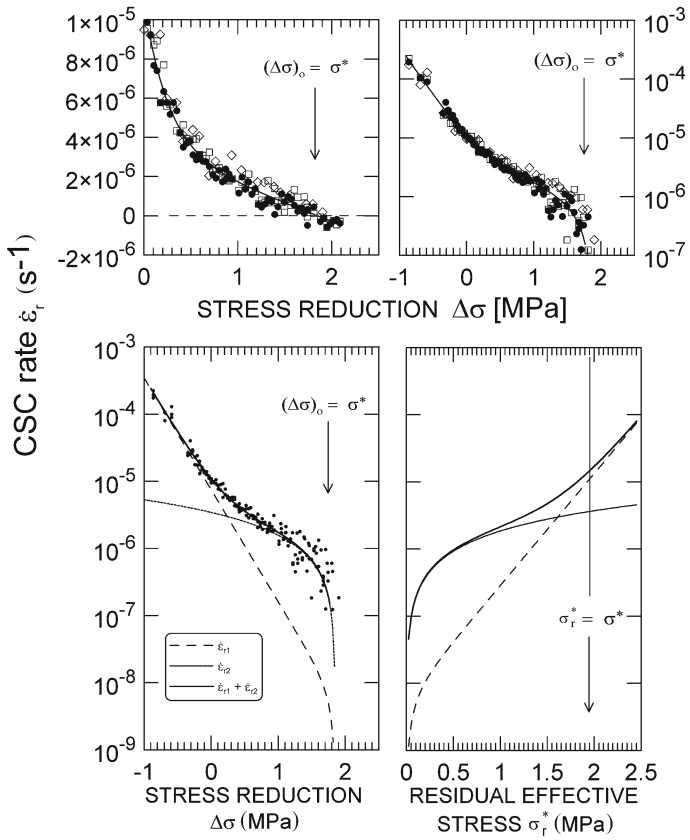

Fig. 4. Example of CSC dependence $\dot{\varepsilon}_\mathrm{r} = \dot{\varepsilon}_\mathrm{r}\,(\Delta\sigma)$ for 573 K and $\sigma = 6.5$ MPa. Various symbols represent the data obtained from treatments of the experiments by three researchers.

of the steady-state creep region was sufficiently long under all experimental conditions so that the CSC dependence $\dot{\varepsilon}_\mathrm{r} = \dot{\varepsilon}_\mathrm{r}(\Delta\sigma)$ for given values σ and T could usually be obtained in single-specimen creep test. A typical example of the dependence $\dot{\varepsilon}_\mathrm{r} = \dot{\varepsilon}_\mathrm{r}(\Delta\sigma)$, which also contains experiments with small negative reductions $\Delta\sigma$, is given in Fig. 4. Beyond the value of the effective stress σ^*, no conclusions can be drawn from the shape of the dependence in the linear coordinates (above, left). The shape of the dependence in semi-logarithmic coordinates (above, right) documents that a simple function consisting of a single sinh term, Eq. (5), cannot describe this dependence in aluminium. Such a function cannot explain convex and subsequent concave segments in the coordinates being used. However, a detailed statistical analysis has shown that the dependences obtained in aluminium can be very well described by means of a function containing two sinh terms, i.e.,

$$\dot{\varepsilon}_\mathrm{r} = A\sinh\left[B\sigma_\mathrm{r}^*\right] + C\sinh\left[D\sigma_\mathrm{r}^*\right] = \dot{\varepsilon}_\mathrm{rI} + \dot{\varepsilon}_\mathrm{rII}, \quad (12)$$

where parameters *A, B, C,* and *D* depend on the external conditions, σ and T. The suitability of the description by this function is confirmed for the presented experiment by the curves in the lower parts of Fig. 4 and further examples, corresponding to various σ and T, illustrated in Fig. 5.

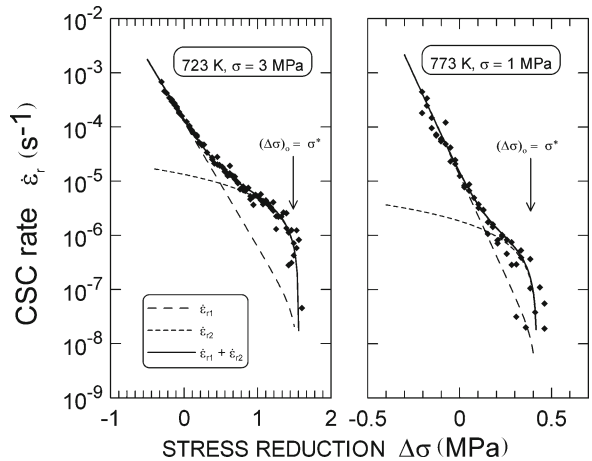

Fig. 5. Description of CSC dependences by Eq. (12) obtained at various temperatures and applied stresses.

It can be – at least formally – assumed that the rate $\dot{\varepsilon}_\mathrm{r}$ as well as the rate $\dot{\varepsilon}_\mathrm{s}$ is composed of two contributions resulting from the two terms of Eq. (12). In order to exclude any misunderstandings in the following considerations, the contribution which dominates

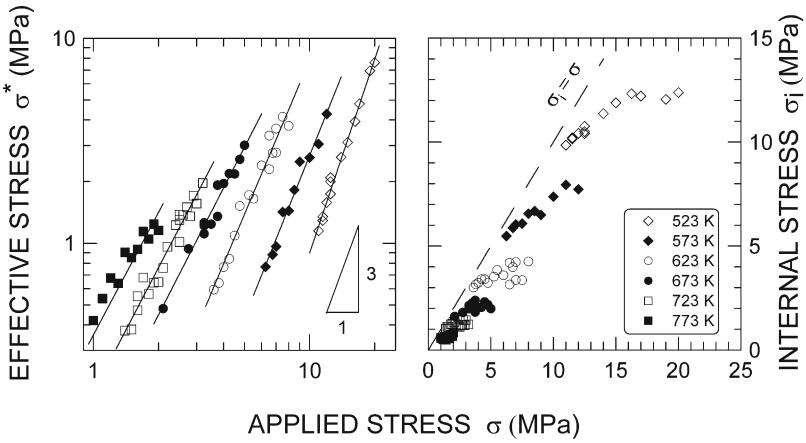

Fig. 6. Applied stress dependences of the effective and internal stresses.

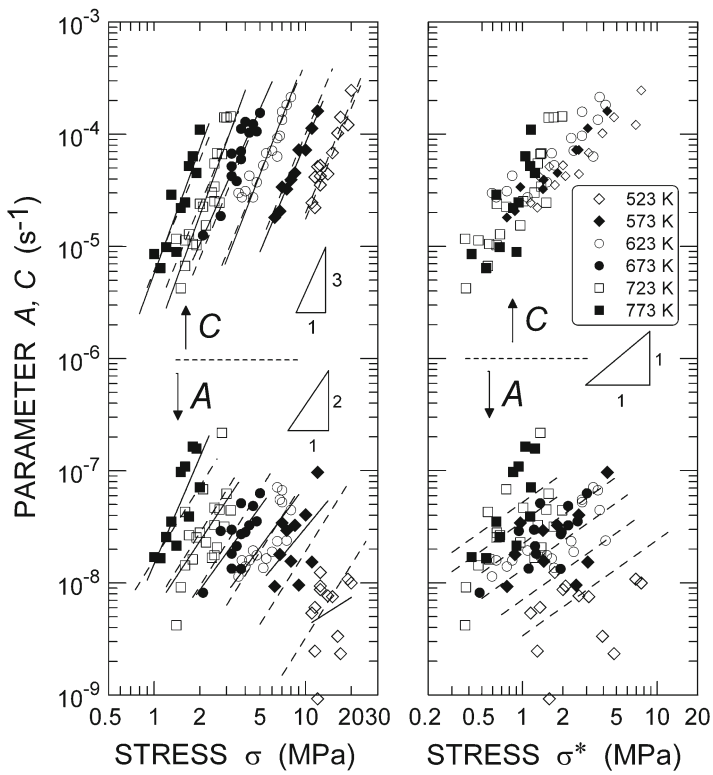

Fig. 7. Dependence of parameters A and C, Eq. (12), on the applied and effective stresses.

at zero and small applied stress reductions $\Delta\sigma$ will be marked by the index I and the relevant parameters are A and B. The second contribution is dominant at greater $\Delta\sigma$. Its index is II and the respective parameters are C and D.

From a set of CSC experiments performed in the course of the steady-state creep under given σ and T, five parameters, i.e. A, B, C, D, and σ^*, are obtained. However, the optimisation of these parameters is not a simple mathematical problem and the determined optimum values of some parameters, namely the parameter A, frequently exhibited large statistical errors as calculated using normal procedures (up to 30 percent). On the other hand, the error of the effective stress σ^* is less than five per cent.

The applied stress and temperature dependences of the effective stress σ^* are plotted in Fig. 6. At a given temperature, the effective stress σ^* increases with increasing applied stress. If a simple power function of the form

$$\sigma^* = p\,(T)\ \sigma^q \tag{13}$$

is used for a description of this dependence, the expo-

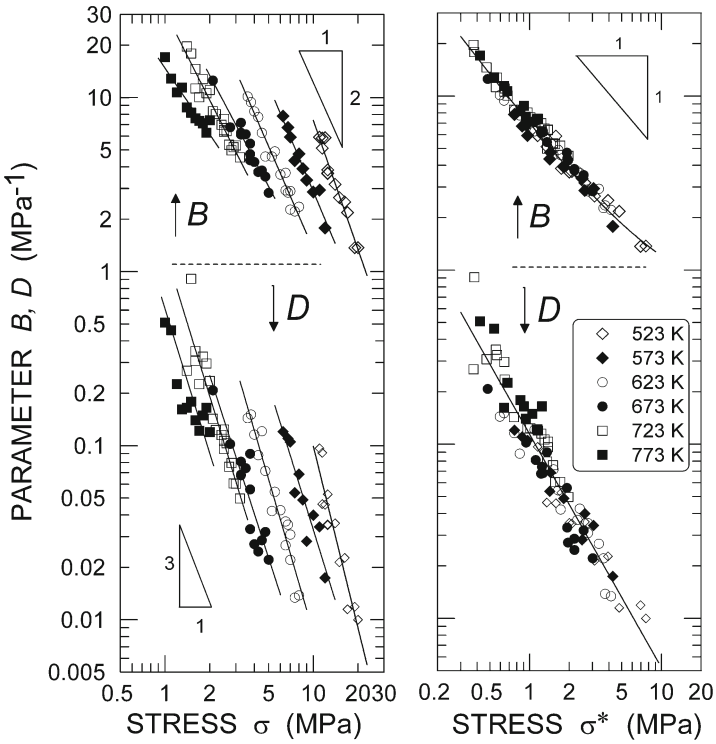

Fig. 8. Dependence of parameters B and D, Eq. (12), on the applied and effective stresses.

nent q reaches the values from two to three at various temperatures. In this figure, the complement of the stress σ^*, i.e., the internal stress σ_i, is also plotted.

The applied and effective stress dependences of parameters A and C are plotted in Fig. 7. The parameter A reaches values from 1×10^{-9} to 2×10^{-7}; the parameter C then ranges from 4×10^{-6} to 3×10^{-4}. Power functions, i.e.,

$$A \propto \sigma^{\omega_A} \quad \text{and} \quad C \propto \sigma^{\omega_C} \tag{14}$$

with constant exponents ω_A and ω_C were used for the description of stress dependence of both parameters. Due to the great scatter of data, no reliable conclusions can be drawn for temperature dependence of the exponent ω_A. On the other hand, the exponent ω_C probably does not depend on temperature. If the combined temperature and applied stress dependence of both these exponents is described by the frequently assumed relationship, i.e.,

$$A \propto \sigma^{\varpi_A} \exp\left[-\frac{\bar{Q}_A}{RT}\right],$$
$$C \propto \sigma^{\varpi_C} \exp\left[-\frac{\bar{Q}_C}{RT}\right], \tag{15}$$

the optimisation of the parameters has yielded values $\bar{Q}_A = 88.3 \pm 8.3\,\mathrm{kJ\,mol^{-1}}$, $\varpi_A = 2.1 \pm 0.3$, $\bar{Q}_C = 87.3 \pm 5\,\mathrm{kJ\,mol^{-1}}$ and $\varpi_C = 3.3 \pm 0.2$. In spite of the great errors in the values of A, the suitability of such a description is apparent from dashed lines drawn in the left section of Fig. 7. The effective stress dependence of parameters A and C can be seen in the right part of Fig. 7. It is apparent that the parameter C either does not depend on temperature at a given stress σ^* or such a dependence is only weak. Again, quite reliable conclusions cannot be deduced for the parameter A due to the relatively great scatter of data. Nevertheless, a description of the combined dependence by the relationship similar to Eq. (15), i.e.,

$$A \propto (\sigma^*)^{\varpi^*_A} \exp\left[-\frac{\bar{Q}^*_A}{RT}\right], \tag{16}$$

gives values $\varpi^*_A = 0.85 \pm 0.15$ and $\bar{Q}^*_A = 37 \pm 4$ $\mathrm{kJ\,mol^{-1}}$. Dashed lines drawn in the plot correspond to these values.

The applied stress dependences of parameters B and D are plotted in the left part of Fig. 8. At a given temperature, both parameters B and D sharply decrease with the increasing applied stress and, at a given stress σ, parameter B increases with decreasing temperature. In comparison with the values of B, parameter D is up to one order in magnitude smaller.

The dependence of D on the applied stress is stronger than that observed for parameter B. If power functions are used for the description of applied stress dependence of both these parameters, then corresponding exponents of the dependence of B and D

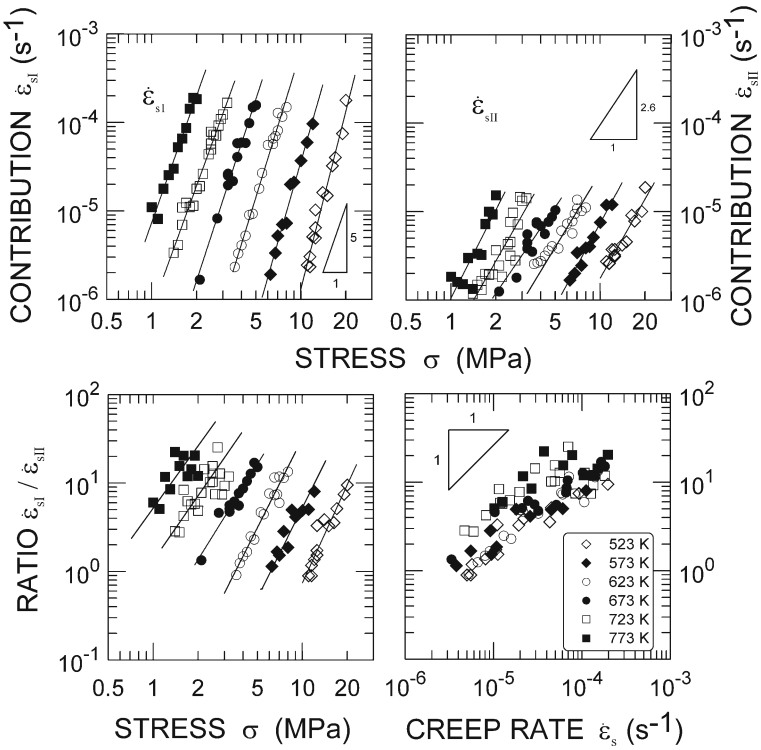

Fig. 9. Contributions of $\dot{\varepsilon}_{\mathrm{sI}}$ and $\dot{\varepsilon}_{\mathrm{sII}}$ to the steady-state creep rate $\dot{\varepsilon}_{\mathrm{s}}$.

are approximately 2 and 3, respectively. The effective stress dependences of both parameters are plotted in the right part of Fig. 8. At a given stress σ^*, neither parameter depends on temperature. While parameter B can be roughly considered proportional to a reciprocal σ^*, parameter D can be described by a power function with an exponent of -1.3.

The behaviour of the contributions $\dot{\varepsilon}_{\mathrm{sI}}$ and $\dot{\varepsilon}_{\mathrm{sII}}$ can be seen in Fig. 9. The applied stress dependences of both contributions at a given temperature, the upper part of the figure, can be well approximated by power functions, i.e. $\dot{\varepsilon}_{\mathrm{sI}} \propto \sigma^{n_1}$ and $\dot{\varepsilon}_{\mathrm{sII}} \propto \sigma^{n_2}$, with values $n_1 \cong 5.0$ and $n_2 \cong 2.5$. If a conjunctive stress and temperature dependence of both contributions in the form

$$\dot{\varepsilon}_{\mathrm{sI}} = K_1 \sigma^{\bar{n}_1} \exp\left[-\frac{\bar{Q}_1}{RT}\right]$$

or (17)

$$\dot{\varepsilon}_{\mathrm{sII}} = K_2 \sigma^{\bar{n}_2} \exp\left[-\frac{\bar{Q}_2}{RT}\right],$$

is used for a description of the data, optimum values $\bar{Q}_1 = 158\,\mathrm{kJ\,mol^{-1}}$, $\bar{Q}_2 = 80\,\mathrm{kJ\,mol^{-1}}$, $\bar{n}_1 = 4.4$, and $\bar{n}_2 = 2.6$ are obtained. For a comparison of the influence of both contributions $\dot{\varepsilon}_{\mathrm{sI}}$ and $\dot{\varepsilon}_{\mathrm{sII}}$ on the steady-state creep rate $\dot{\varepsilon}_{\mathrm{s}}$, the applied stress and steady-state creep rate dependences of their ratio $\dot{\varepsilon}_{\mathrm{sI}}/\dot{\varepsilon}_{\mathrm{sII}}$ are plotted in the lower part of the figure. This ratio depends on temperature as well as on the applied stress. The dominance of the contributions $\dot{\varepsilon}_{\mathrm{s1}}$ weakens with decreasing applied stress at a given temperature. Both contributions are comparable at the lowest experimental temperature and applied stresses. However, the ratio $\dot{\varepsilon}_{\mathrm{sI}}/\dot{\varepsilon}_{\mathrm{sII}}$ does not differ substantially at a given value of the rate $\dot{\varepsilon}_{\mathrm{s}}$ and various temperatures. Approximately at rates $\dot{\varepsilon}_{\mathrm{s}} \leq 3 \times 10^{-6}\,\mathrm{s^{-1}}$, the ratio is lower than 1 and the contribution $\dot{\varepsilon}_{\mathrm{sII}}$ becomes dominant.

5. Discussion

5.1. Applied stress and temperature dependences of the steady-state creep rate

The applied stress and temperature dependences of the steady-state creep rate $\dot{\varepsilon}_{\mathrm{s}}$ do not differ substantially from the dependences obtained by other authors who investigated creep behaviour of aluminium under similar experimental conditions, see e.g. [11]. Therefore, a conventional analysis of the applied stress and temperature dependences of the rate $\dot{\varepsilon}_{\mathrm{s}}$ obtained in the present work yielded activation characteristics, i.e., the applied stress sensitivity parameter n and the activation energy Q_{C}, Eqs. (10) and (11), which correspond well to the values usually observed. Thus, the present data lead to the same conclusions obtained by other authors using con-

ventional procedures of steady-state creep analysis of aluminium. Such a conclusion can be considered significant from the point of view of the present work's aims.

5.2. Constant structure creep

A procedure based on an assumption of the decisive role of the residual effective stress σ_r^* in the constant structure creep will be applied in the following analysis of the CSC data. The basic assumptions of this procedure were summarised in Section 2. The CSC dependences $\dot{\varepsilon}_r = \dot{\varepsilon}_r(\Delta\sigma)$ obtained in the steady-state creep are very well described by Eq. (12) over the whole experimental interval of applied stresses and temperatures. The possibility of describing CSC, i.e., a description by means of two sinh terms, has already been reported for steady-state creep in aluminium [12] and was used for describing CSC in the primary stage of creep of several metallic materials [10]. A detailed discussion of such a description resulted in a suggestion of the simultaneous activity of two independent mechanisms, which contribute to the total creep rates $\dot{\varepsilon}_r$ and $\dot{\varepsilon}_s$ [10]. Such an assumption is not very surprising. The existence of two mechanisms can result, e.g., from the existence of two basic types of dislocations, from the two-phase structure developed in single phase crept metals and alloys, etc. The existence of two mechanisms acting in creep of aluminium has also been demonstrated by Blum et al. [2].

In principle, a procedure identical to that, which was used for interpreting the one sinh term description, can be applied to the interpretation of each of these two sinh terms. Parameters of each of these terms can be then interpreted by characteristics of the corresponding mechanism. However, a serious objection can be raised against the specific form of Eq. (12), namely against the assumption of identical values for the effective stress σ^* for both mechanisms. The possibility of different effective stresses for these mechanisms and the consequences resulting from such a possibility were discussed previously [10]. The assumption of common effective stress for both mechanisms is the only possibility of explaining the physical nature of the parameters of Eq. (12). Therefore, identical values of the effective stresses for both mechanisms will be assumed in following considerations.

The dependences of the effective and internal stresses on the applied stress and temperature, Fig. 6, do not differ qualitatively from the usually observed dependences in other single-phase materials, e.g. [13]. Any detailed analysis of these dependences leading to an explanation of the nature of these stresses could not be disputed without extensive and systematic structure investigations of the crept specimens and their analysis. For the following considerations, the assumptions that the effective stress is the driving stress and the internal stress is the quantity characterizing structure, are sufficient.

In accordance with the suggested procedure, the parameters A, B, C, D, and σ^* in Eq. (12) are connected with the characteristics of the relevant mechanisms, namely with the density of moving dislocation ρ_m, the free energy ΔF of obstacles and the activation area a^*, by the relationships:

$$A \propto \rho_m^{I} \exp\left[-\frac{\Delta F^{I}}{RT}\right], \quad B = \frac{a_I^* b}{RT} \tag{18}$$

for the first mechanism, and

$$C \propto \rho_m^{II} \exp\left[-\frac{\Delta F^{II}}{RT}\right], \quad D = \frac{a_{II}^* b}{RT} \tag{19}$$

for the second mechanism.

The applied stress dependence of the parameter A, Fig. 7, can be described by a power function at a given temperature, Eq. (14). Even if the experimental scatter of the data is relatively large, it can be assumed that the exponent ω_A is either greater than or equal to 2 at all experimental temperatures and it probably slowly increases with increasing temperature. The optimisation of the data using Eq. (15) has given a mean value of the exponent $\varpi_A \approx 1.7$. According to Eq. (18), the stress dependence of parameter A is given by the dependence of the dislocation density ρ_m^{sI}. A power relationship with the exponent ≈ 2 is quite acceptable from the point of view of the commonly accepted applied stress dependence of the moving dislocation density ρ_m in single-phase metallic materials [14]. The experimental energy $\bar{Q}_A \approx 76\,\mathrm{kJ\,mol^{-1}}$ results from the expression of the temperature dependence of parameter A described by Eq. (15). The temperature dependence of parameter A at a given applied stress should result from both terms, i.e., from density ρ_m^{sI} and $\exp\left[-\frac{\Delta F^{I}}{RT}\right]$. It follows from the above procedure that the experimental value of $\bar{Q}_A$ can characterise either the free energy of obstacles in the generation of mobile dislocation or obstacles to their motion or – possibly – both these phenomena. In principle, these components are inseparable within the value $\bar{Q}_A$. Given the fact that the dependence of the total density of dislocation ρ_t on temperature is generally rather weak in most single-phase metallic materials [14] and given the frequently accepted assumption of a close relation between ρ_m and ρ_t (proportionality), the dominant influence of free energy for obstacles in the dislocation motion on the temperature dependence of parameter A is acceptable also for mechanism I. Based on this assumption, the motion of dislocations is characterised by the energy $\bar{Q}_A \approx 76\,\mathrm{kJ\,mol^{-1}}$, and

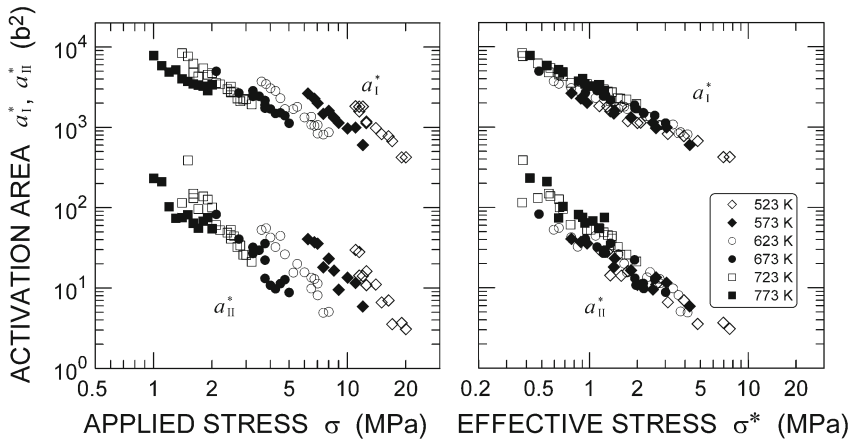

Fig. 10. Applied and effective stress dependence of activation areas a_{I}^* and a_{II}^*.

this value must be discussed from the point of view of possible mechanisms of dislocation motion. If a mechanism controlled by a diffusion process is considered, only mechanisms connected with the high diffusivity path may be taken into account. Because of the value of $\bar{Q}_{\mathrm{A}} \approx 0.6\ \Delta H_{\mathrm{L}}$, diffusion along the dislocation cores should be the most probable controlling process of the relevant mechanism of the dislocation motion (mechanism I). Values from 0.5 to 0.7 ΔH_{L} correspond to the activation enthalpy of this type of diffusion, see e.g. [11].

Further information concerning the mechanism I, namely the activation area a_{I}^*, can be obtained from parameter B, Eq. (18). Both dependences of the area a_{I}^* on the applied and effective stresses are plotted in Fig. 10. From the point of view of dislocation kinetics, the relevant stress variable for considerations concerning the dislocation glide mechanisms is the effective stress σ^*[15]. The results obtained fully support such an assumption. While the dependences $a_{\mathrm{I}}^* = a_{\mathrm{I}}^*(\sigma)$ differ for various temperatures, the dependences $a_{\mathrm{I}}^* = a_{\mathrm{I}}^*(\sigma^*)$ probably coincide. The area a_{I}^* reaches values from approximately 10^3 to 10^4 b^2. It should be emphasised that this value must be understood only as an apparent quantity; the true activation area a_{I}^* is greater than that experimentally determined, at least about the Taylor factor $M \cong 2$. At a given temperature, the area a_{I}^* is proportional to the reciprocal effective stress and, at a given σ^*, it slowly increases with increasing temperature. Thus, the dislocation mechanism I, which dominates in the steady-state creep and at small applied stress reductions in the CSC, is characterised by the activation area a_{I}^* ranging from 10^3 to 10^4 b^2, and is probably governed by core diffusion. The explicit assignment of some known dislocation mechanisms to such parameters is very questionable. From previously suggested simple models of creep, the model of non-conservative slip of jogged screw dislocations may conform to such parameters, see e.g. [13] for more details. In such a

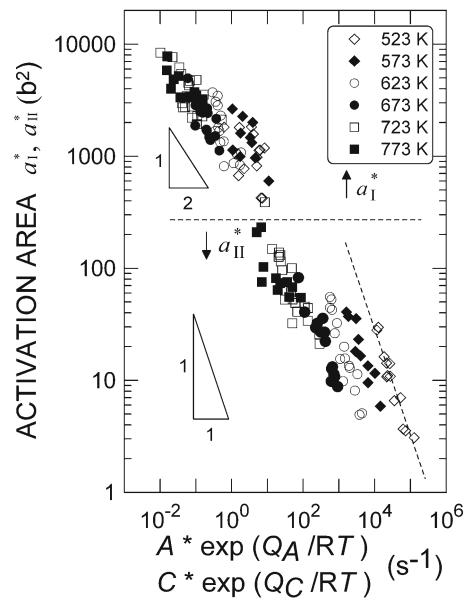

Fig. 11. Relations between activation areas a_{I}^* and a_{II}^* and temperature-compensated parameters A and C.

case, the average distance between the neighbouring jogs lies between 10^3 to 10^4 b and the diffusion of vacancies runs along the core of the moving dislocation. Note that the decisive role of diffusion along the dislocation cores is quite plausible for this mechanism.

However, cross slip mechanisms should also be considered as possible controlling processes of creep in addition to diffusion-controlled mechanisms. Unfortunately, no detailed data concerning the free activation energies and the activation areas of these mechanisms in aluminium are available for a comparison of the relevant activation parameters.

A discussion of the parameters of mechanism II corresponding to the second term of Eq. (12) yields conclusions qualitatively very similar to those obtained for mechanism I. The description of parameter

C using Eq. (16) gives an optimum value of the activation energy $\approx 72\,\mathrm{kJ\,mol^{-1}}$, which is very close to the value of $\bar{Q}_\mathrm{A}$ for mechanism I. Therefore, similar conclusions can be derived about the controlling process of the mechanism II, i.e., diffusion along dislocation cores can be suggested as the most probable process in the case of the controlling role of diffusion processes in creep. In contrast to mechanism I, the activation area a^*_II is approximately up to two orders of magnitude lower than area a^*_I, see Fig. 10. The area a^*_II is also proportional to the reciprocal effective stress σ^* and, at a given σ^*, it probably only slowly increases with increasing temperature. Apparently, such events might be relevant more likely to subboundaries. Blum et al. [2] suggested a mechanism controlled by recovery processes near subgrain boundaries as the probable mechanism. The activation energy $\bar{Q}_\mathrm{C}$, which is close to the value of the enthalpy of core dislocation diffusion, should support such suggestion. From the energetic point of view, this type of diffusion is more convenient than lattice diffusion usually connected with recovery processes. However, in accord with contemporary models of two-phase structure, the value of the effective stress must be also discussed.

An acceptance of the results of CSC procedure offers a possibility of deducing some further suggestions.

First, qualitative relationships between the moving dislocation density $\rho^\mathrm{s}_\mathrm{m}$ and activation area a^* can be deduced for both mechanisms. With respect to Eqs. (18) and (19), it can be approximately written $\rho^\mathrm{sI}_\mathrm{m} \propto A\exp\left[\bar{Q}_\mathrm{A}/RT\right]$ and $\rho^\mathrm{sII}_\mathrm{m} \propto C\exp\left[\bar{Q}_\mathrm{C}/RT\right]$. The dependences of activation areas a^*_I and a^*_II on these two products are plotted in Fig. 11. Despite the great experimental scatter of parameter A, it is apparent that the relationship $a^*_\mathrm{I} = a^*_\mathrm{I}\left(\rho^\mathrm{sI}_\mathrm{m}\right)$ is probably not influenced by temperature and, in a good approximation, it can be described as $a^*_\mathrm{I} \propto \sqrt{\rho^\mathrm{sI}_\mathrm{m}}$. In contrast to this, the relationship $a^*_\mathrm{II} = a^*_\mathrm{II}\left(\rho^\mathrm{sII}_\mathrm{m}\right)$ is influenced by temperature, at least in its lower values. The dependence of a^*_II on reciprocal $\rho^\mathrm{sII}_\mathrm{m}$ is probably linear at a given temperature.

Second, it must be pointed out that the contribution of mechanism I to the steady-state creep rate $\dot{\varepsilon}_\mathrm{s}$ is dominant, and, therefore, it determines the rate $\dot{\varepsilon}_\mathrm{s}$ over almost the whole experimental interval. On the other hand, the phenomenological activation parameters, e.g., the apparent activation energy Q_app and the stress sensitivity parameter n must include corresponding contributions of both mechanisms. The relations between the apparent experimental values of these parameters and the corresponding values for separate mechanisms can be derived.

Third, note that the existence of two creep mechanisms resulting from the CSC experiments and the resulting applied stress and temperature dependences of the ratio $\dot{\varepsilon}_{\mathrm{s}1}/\dot{\varepsilon}_{\mathrm{s}2}$ explains in a plausible way the power break which is observed in applied stress dependences of the rate $\dot{\varepsilon}_\mathrm{s}$ at lower stresses σ in aluminium, see e.g. Blum and Maier [16].

Finally, the existence of two independent mechanisms acting in the steady-state creep may also explain the relatively unsuccessful interpretation of CSC results by means of Eq. (2). A detailed analysis of CSC dependences obtained in this work has shown that the assumption of a simple exponential shape of the CSC dependence in the interval of small stress reductions $\Delta\sigma$ is not valid over virtually the whole range of experimental conditions σ and T. The segment of the dependence for small reductions $\Delta\sigma$ is convex.

Any further deductions aimed at suggesting the nature of both these mechanisms based only on the present results may be disputed. A necessary next step in the investigations could consist of a detailed quantitative structure analysis, which should be directed at verifying the above-suggested conclusions. However, even such analysis should be performed by *in situ* structure investigations, which is difficult by contemporary standard of experimental techniques.

6. Conclusions

Investigations of creep behaviour of aluminium in a temperature interval from 523 to 773 K yielded following conclusions:

- From a conventional analysis of the applied stress and temperature dependences of the steady-state creep rate $\dot{\varepsilon}_\mathrm{s}$, conclusions can be drawn similar to those obtained by other authors.
- The application of constant structure creep experiments in the steady-state stage of creep has shown that

– the creep rate $\dot{\varepsilon}_\mathrm{s}$ can be considered to be the result of two creep mechanisms. One of these mechanisms is dominant over a substantial part of the whole range of experimental conditions ($\dot{\varepsilon}_\mathrm{s} \geq 10^{-6}\,\mathrm{s^{-1}}$). If a diffusion process controls the steady-state creep, then both mechanisms are probably governed by diffusion along the high diffusivity path, most probably by diffusion along the dislocation cores. The activation areas of the mechanisms differ substantially. While the activation area of the dominant mechanism reaches values from 10^3 to 10^4 b^2 and the density of dislocations moving by it is proportional to the square of the applied stress, the activation area of the minor mechanism is two orders of magnitude lower and the density of dislocation moving by this mechanism depends on the third power of the applied stress.

– an application of CSC procedure offers alternative possibilities for the investigation of physical bases of deformation processes in steady-state creep in aluminium.

Acknowledgements

The work was supported by the Grant Agency of the Academy of Sciences of CR under contract A2041203. The author is indebted to J. Slaměníková and Dr. V. Floriánová for valuable cooperation in extensive experiments and in evaluation of their results.

References

[1] VOGLER, S.—BLUM, W.—BIBERGER, M.—MUKHERJEE, A. K.: Mater. Sci. Engng., *A112*, 1989, p. 93.
[2] BLUM, W.—ROSEN, A.—CEGIELSKA, A.—MARTIN, J. L.: Acta Metall., *37*, 1989, p. 2439. doi:10.1016/0001-6160(89)90041-2
[3] NAKAYAMA, G. S.—GIBELING, J. C.: Acta Metall., *38*, 1990, p. 2023. doi:10.1016/0956-7151(90)90314-7
[4] DOBEŠ, F.: Scripta Metall. Mater., *27*, 1992, p. 1435. doi:10.1016/0956-716X(92)90097-X
[5] MILIČKA, K.: Acta Metall. Mater., *41*, 1993, p. 1163. doi:10.1016/0956-7151(93)90164-N
[6] AHLQUIST, C. N.—NIX, W. D.: Scripta Metall., *3*, 1969, p. 679.
[7] SHERBY, O. D.—KLUNDT, R. H.—MILLER, A. K.: Metall. Trans., *8A*, 1977, p. 843.
[8] KOCKS, U. F.—ARGON, A. S.—ASHBY, M. F.: Thermodynamics and Kinetics of Slip. Oxford, Pergamon Press 1975.
[9] DOBEŠ, F.—MILIČKA, K.: Scripta Mater., *38*, 1998, p. 1797.
[10] MILIČKA, K.: Acta Metall. Mater., *42*, 1994, p. 4189. doi:10.1016/0956-7151(94)90195-3
[11] FROST, H. J.—ASHBY, M. F.: Deformation-Mechanism Maps. Oxford, Pergamon Press 1982.
[12] MILIČKA, K.—DOBEŠ, F.—SLAMĚNÍKOVÁ, J.: Mater. Sci. Engng., *A234–236*, 1997, p. 912.
[13] ČADEK, J.: Creep in Metallic Materials. Praha – Amsterdam, Academia – Elsevier 1988.
[14] TAKEUCHI, S.—ARGON, A. S.: J. Mater. Sci., *11*, 1976, p. 1542. doi:10.1007/BF00540888
[15] MULFORD, R. A.: Acta Metall., *27*, 1979, p. 115.
[16] BLUM, W.—MAIER, W.: phys. stat. sol. (a), *171*, 1999, p. 467.